Ecological Modelling 514 (2026) 111497

Contents lists available at ScienceDirect

Ecological Modelling

journal homepage: www.elsevier.com/locate/ecolmodel

Estimating the yield of Parkia biglobosa fruits from field data and image-based predictive models

Franklin X. Dono [a,b,c,*], Bernard N. Baatuuwie [a,d], Anne Mette Lykke [e], Felix K. Abagale [a], Peter Borgen Sørensen [e]

[a] *West African Center for Water Irrigation and Sustainable Agriculture (WACWISA), University for Development. Studies, Tamale, Ghana*
[b] *Department of Environmental Management and Sustainability, University for Development Studies, Tamale, Ghana*
[c] *Ghana Atomic Energy Commission (GAEC), Nuclear Power Institute (NPI), Legon, Accra-Ghana*
[d] *Department of Natural Resources and Geo-Information Sciences, Faculty of Natural Resources and Environment, University for Development. Studies, Tamale, Ghana*
[e] *Institute of Ecoscience, Faculty of Technical Sciences, Aarhus University, Aarhus, Denmark*

ARTICLE INFO

Keywords:
Remote sensing
Yield estimation
Mathematical Modelling
Soil Properties
Morphology

ABSTRACT

Accurate estimates of tropical tree fruit yields are essential for assessing individual tree productivity and landscape-scale applications. This study examines the productivity of *Parkia biglobosa* pods by integrating tree morphology, vegetation health indices from drone and satellite images, and soil properties into a mathematical model. The model evaluates interactions between these factors and their contribution to yield. Fruits were harvested from 105 mature trees within three study sites in the savanna ecological zones of Ghana and weighed. The crown radius of selected trees was measured in meters from mosaics derived from drone images in QGIS. Satellite images and data on the physical and chemical soil properties were obtained from the Norway International Climate and Forest Initiative (NICFI) and the Soil Reference and Information Centre (ISRIC), respectively. The yield was estimated by an exponential relationship involving the tree crown radius, average blue band reflectance from satellite images, and interaction with the locality. The model explained 75 % of the variation in yield. Excluding interaction terms, the best model estimated yield from tree crown radius, average near infrared reflectance of the crown, and soil pH at 30 – 60 cm depth. It indicated that crown radius, soil pH, Blue and Near-infrared spectral characteristics, along with variations in locality, such as soil and tree management practices, influenced the yield of *Parkia biglobosa*. Collectively, they explained 67.8 % of the variation in the yield. Policies to control tree stand undergrowth, prevent bushfires, promote less invasive harvesting techniques, and monitor soil nitrogen and pH levels are recommended for localities to enhance tree health and productivity.

1. Introduction

Accurate estimates of tropical tree fruit yields are essential for the socioeconomic development of many African countries. These yield estimates help to assess the productivity of individual trees, implement effective management practices, and estimate market supply in the face of changing climatic conditions. Therefore, a solid understanding of the factors that influence yield is crucial for making improved yield predictions under various conditions. Morphology, soil properties, management practices, and local climatic conditions determine the yields of trees. Tree morphological variables were utilized by Liu et al., (2023) for non-destructive biomass assessment of tropical trees, demonstrating the importance of structural characteristics in understanding tree productivity.

Spectral properties of the crown may disclose the health condition of the tree and thus properties relevant for the yield of fruit harvest. Recent advancements in global positioning systems (GPS), geographic information systems (GIS), remote sensing, and drone technology have improved landscape visualization and governing factors (Asad Naqvi and Naqvi, 2022). These technologies, combined with yield data, allow for better prediction of yield. Tree traits and climate are important predictors of production, which can be estimated accurately from remotely sensed images (Panagiotidis et al., 2017) by both manual and automated methods (Area and Photographs, 2004). In several cases, there has been considerable success in predicting yield with spectral indices (Panda et al., 2010). For instance, cotton yields have been

* Corresponding author.
E-mail address: frankxdonox@gmail.com (F.X. Dono).

https://doi.org/10.1016/j.ecolmodel.2026.111497
Received 15 September 2025; Received in revised form 12 January 2026; Accepted 14 January 2026
Available online 22 January 2026

accurately estimated from spectral indices and texture features derived from RGB images (Yiru et al., 2022).

Plant traits influence the spectral signals captured by drones and satellites, enabling studies on vegetation health, production, distribution, and functionality over large areas (Hauser et al., 2021; Houborg et al., 2015; Ma et al., 2019; Thomson et al., 2018). Variation in tree leaf color, shape, canopy cover (Ribeiro da Luz and Crowley, 2010), and yield (Apolo-Apolo et al., 2020; Barbosa et al., 2021) can be determined from spectral characteristics.

In contrast to spectral signals, which provide indirect measures of vegetation health and productivity through indices derived from reflectance patterns, tree traits provide direct insights into tree yield. The tree growth rate, annual circumference, and wood density are key traits that can significantly influence the productivity and yield of trees (Prado-Junior et al., 2016). The impact of these traits on the tree yields can vary based on human pressure, climatic, and management conditions (Prado-Junior et al., 2016).

In the case of the *Parkia biglobosa,* which is a multipurpose native tree heavily depended on by folks for its nutritional, health, and socio-economic benefits, estimating its annual production of fruits is a challenge due to human pressure (Prado-Junior et al., 2016) and climate change. Fruits are randomly harvested and used by local people, hindering systematic data collection (Houndonougbo et al., 2020). However, pod yield is correlated with crown diameter and diameter at breast height, though stronger with crown diameter, and it fluctuates significantly across years due to climate and management practices (Bokary et al., 2022).

Among savanna shrub species in West Africa, crown volume is the stronger predictor of fruit production than stem diameter, with larger trees yielding more fruits under climate influence (Ounyambila et al., 2018). In their model, Ounyambila et al., (2018) incorporated climatic factors, and this research extends their approach by adding both soil, drone, and satellite spectral characteristics to assess the fruit yield of *Parkia biglobosa* using a modified version of their model.

While significant research exists on yield, tree form, vegetation health, climate, and soil, the factors are rarely integrated into a unified framework for yield studies. This study combines tree form, vegetation health indices (from drone and satellite images), and existing soil variables into a mathematical model to wholistically assess their interactions and contribution to the yield of *Parkia biglobosa* pods, and to assess the potential for larger-scale applications. Thus, the study intends to address the challenges in the yield estimation of this multipurpose native tree to help estimate market supply and implement sustainable management practices in the face of changing climatic conditions.

2. Materials and methods

2.1. Study area

The study was conducted in three sites in northern Ghana: Nandom

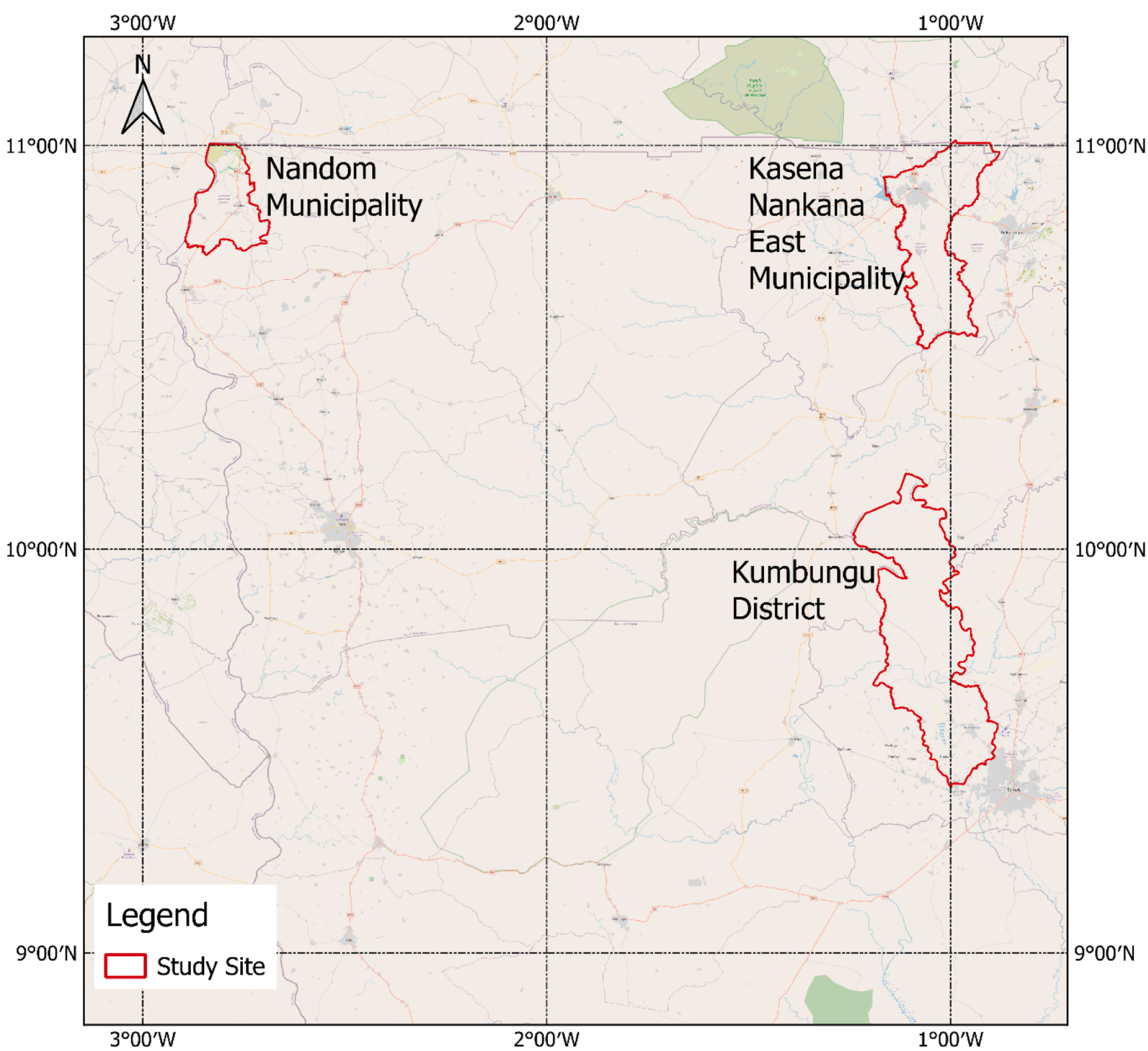

Fig. 1. Geographical location of study sites in northern Ghana. (Note: map lines delineate study areas and do not necessarily depict accepted national boundaries).

Municipality (2°41′-2°54′ W and 10°44′-11°00′ N) in the Upper West Region, Kasena-Nankana East Municipality (1°10′-0°53′ W, and 10°30′-11°01′ N) in the Upper East Region, and Kumbungu District (1°14′-0°53′ W and 09°25′-0°11′ N) in the Northern Region (Fig. 1).

The study areas experience a unimodal rainfall pattern from May to October. Average annual rainfall varies by location, with Nandom receiving approximately 999 mm, Kasena-Nankana 1002 mm, and Kumbungu 1078 mm. The monthly average temperatures are 28.9°C in Nandom, 29.1°C in Kasena-Nankana, and 28.8°C in Kumbungu (Harris et al., 2020).

The soil types common to all three study areas are Lixisols and Fluvisols. In addition, Nandom has Arenosols and Vertisols, Kasena-Nankana has Leptosols, and Kumbungu has Planosols, Plinthosols, and Acrisols (Soil Research Institute, 1999). Coupled with erosion, a widespread phenomenon, the various soil types vary in their sand and clay content.

Agriculture is the primary economic activity supported by the soils in the study areas. Most households are involved in subsistence farming, growing crops such as millet, sorghum, maize, and groundnuts (Nandom Municipal Assembly, 2016). Additionally, livestock contributes extra income and food. The trade of *Parkia biglobosa* (locust bean) is particularly important for livelihood support. During the dry season, bushfires threaten *Parkia biglobosa* by damaging both seedlings and trees. The impact on yield loss is exacerbated by climate change and poor land management practices.

2.1.1. Study species

Parkia biglobosa is common in the Sudanian zones up to the edge of the Sahel in West and Central Africa and occurs in savanna fields, and fallows. It is a deciduous tree up to 20–30 m high, and it belongs to the family Fabaceae (Komolafe et al., 2024). It starts fruiting at the age of eight years and yields 25-100 kg of pods/tree/year when it is 15 to 20 years old (Pasiecznik, 2022). The fruit is a slightly curved, brown indehiscent pod, 30-40 cm long and 2-3 cm wide. It produces 5 to 20 seeds per pod (Ayanrinde et al., 2023).

2.2. Field sampling data

Matured trees of *Parkia biglobosa* were sampled from the three study sites, using an approach where 105 trees were randomly selected from 300×300-meter grid layouts in settlements with relatively high tree density. There were 32 trees in Kumbungu, 49 in Nandom, and 24 in Navrongo, which were geotagged for easy tree identification on orthomosaic images derived from drone flight missions. Harvesting was between March and April when the pods turned brown and dry. All fruits were harvested using climbing and sickle-plucking techniques, then weighed in situ to determine the yield per tree in kilograms.

2.2.1. Drone images

The sites were overflown with the DJI mini 2 drone equipped with 12-megapixel RGB (red, green, blue) sensors of focal length 35 mm. Flight missions were planned and completed the last week before the harvest date using Dronelink software (Dronelink, 2022). Forward and lateral overlaps were 80 % and 70 %, respectively. Images were automatically geotagged using the onboard global positioning system.

The images were used to derive orthomosaic maps. *Parkia biglobosa* populations were identified on the maps by their location coordinates. The crown area for an identified tree was measured in square meters by calculating the area of a polygon delineated around the crown in QGIS. The red, green, and blue spectral bands were extracted, and their average values were calculated as R.x, G.x, and B.x, respectively. In addition, tree health indices-Normalized Green Red Difference Index (NGRDI), Green Leaf Index (GLI), Simple Ratio (SR), Chlorophyll Index (CI), Brightness, Greenness, Wetness were calculated, and their impact on yield was investigated together with the crown radius and soil parameters.

2.3. Satellite images, climate, and soil data

Weekly satellite images from the Norway International Climate and Forest Initiative (NICFI) satellite data program with 5-meter resolution were obtained at most one month (4 weeks) before the harvest date. The images were composited to reduce cloud effects. Cloud-free images were prioritized when available. Tree health indices were computed from the images. The boundary shapefiles for the study sites were used to extract the red, green, blue, and near-infrared bands. Averages for the red, green, blue, and near-infrared bands were calculated for each crown region as R.y, G.y, B.y, and N, respectively. The Normalized Difference Vegetation Index (NDVI) was calculated in addition to the previous indices differentiated by suffix ".x" and ".y" for commonly named drone and satellite indices, respectively.

Macro climatic variables were extracted from the gridded Climatic Research Unit Time-series data version 4.07 (Harris et al., 2020). The data contained month-by-month variations in precipitation and daily mean temperature from 1901 to 2022 on 0.5° x 0.5° grids. The boundary shapefiles were used to extract precipitation and temperature values for the three study areas. They were filtered for records within the year preceding the year 2023 and used to construct annual mean precipitation and temperature metrics.

Soil data was obtained from a global soil data product (SoilGrids) generated by the International Soil Reference and Information Centre (ISRIC) at six standard depth intervals and a spatial resolution of 250 meters (Poggio et al., 2021). Using the tree locations, the soil sand, clay, and silt content, nitrogen, soil pH in water (pH), bulk density (BD), cation exchange capacity at pH 7 (CEC), Coarse fragments volumetric (CFVO), and soil organic carbon (SOC) were extracted at intervals from a depth of 5 to 200 centimeters and their impact on yield was investigated.

2.4. Relationships modelling

Tree productivity increases nonlinearly with crown size because larger crowns intercept more light for photosynthesis (Duursma and Mäkelä, 2007; Garden, 2017; Pretzsch, 2014). A linear model, however, assumes a constant marginal gain per unit radius, which does not account for the effect of changes in the three-dimensional shape of the crown.

We assumed that the yield per tree (measured in kilograms) exhibited a nonlinear relationship with crown radius, where doubling the crown radius resulted in a greater-than-proportional increase in yield. This assumption reflects the three-dimensional nature of the crown structure, where increases in diameter lead to exponential increases in crown volume and hence yield. Again, we expected trees of different sizes to produce varying amounts of harvest, with larger trees showing more variation in their production than smaller trees. To simplify this complex relationship, the model utilized logarithms to transform it into a linear relationship, as described below.

The yield of a tree was modelled as a product of the global yield coefficient term, explanatory variable predictors (drone-based spectral indices, satellite-based spectral indices, and soil properties), categorical variable (location, climate, etc.), and interaction terms. These were analyzed using Ordinary Linear Least Squares (OLS) models of the logarithmic yield as a function of variables and their interactions. The generalized exponential model was specified as:

$$Y_j = \beta_0 \cdot r^n \cdot \prod_{i=1}^{I} \left[e^{\beta_i \cdot X_i} \right] \cdot f(Location, interactions) \tag{1}$$

$$Y_j = \beta_0 \cdot r^n \cdot \prod_{i=1}^{I} \left[e^{\beta_i \cdot X_i} \right] \cdot e^{\left(\gamma_j + \sum_{k=1}^{I} \alpha_{jk} \cdot X_k \right)} \tag{2}$$

Where Y represents the yield of the tree and the global coefficient β_0 provides the baseline yield estimate. The global term $\beta_0 \cdot r^n$ estimates the expected yield from a tree with crown radius r, representing a global mean value. The exponent n is a scaling factor between the canopy radius and yield. It quantifies how efficiently changes in canopy structure translate into fruit yield: when n=2, yield is proportional to the surface area of an ideal spherical crown, and when n=3, yield is proportional to the crown volume. The fitted n value adjusts for structural traits.

X_i represents the i^{th} variable in a set of total i explanatory variables, with β_i as the coefficient, quantifying the influence of the variable X_i on the yield Y. These variables include factors like soil properties, climate, and spectral characteristics of the crown, which may influence or indicate yield. Each location has its own coefficient $\gamma_{j,}$ quantifying its influence on yield, for location j, where the total number of locations is J. The variable α_{jk} models the interaction between explanatory variables X_k X_k (e.g., drone, satellite, soil) and the location.

The logarithm model is derived from Equation 2 as

$$\ln(Y_j) = \ln(\beta_0) + n \cdot \ln(r) + \sum_{i=1}^{I} \beta_i \cdot X_i + \gamma_j + \sum_{j=1}^{J} \sum_{k=1}^{I} \alpha_{jk} \cdot X_k \ldots \tag{3}$$

Estimating interaction coefficients α_{jk} can be challenging if the dataset does not sufficiently capture all combinations of location X_i values. In such cases, neglecting the interactions simplified Equation 3 to:

$$\ln(Y_j) = \ln(\beta_0) + n \cdot \ln(r) + \sum_{i=1}^{I} \beta_i \cdot X_i + \gamma_j \tag{4}$$

Since $\ln(\beta)$ is a constant, it can be replaced with β_0' for all practical purposes

Typically, the variation due to X_i and between locations and individual trees as reflected by the β_i and γ_j values will not be highly dominant, therefore, the Taylor approximation of the exponential function ($e^x \approx 1 + x$) for small numeric values of x is useful for inference as:

$$Y_j \approx \beta_0 \cdot r^n \prod_{i=1}^{I} (1 + \beta_i \cdot X_i) \cdot \left(1 + \gamma_j\right) \tag{5}$$

Hence, if the effect of location j is γ_j=0.2, then the location is approximately 20 % higher in yield compared to the other location under the same conditions for all other factors and for the same size of tree. Where γ_j are the coefficients corresponding to each location.

Interactive-Form-Models were specified out of Equation 3 to include soil, drone, and satellite-based parameters, location, and their interactions (Appendix A). Basic-Form-Models (models without interaction terms) were also specified from Equation 4 (Appendix B).

2.4.1. *Selection and validation of models*

A series of simple OLS models combining the global term with different drone, satellite, and soil variables were used to avoid model overfitting (Madin and Nelson, 2023). A repeated random sampling of data with a holdout for final validation was adopted for model selection (Appendix C).

The selected models were used to estimate yield on the validation dataset and evaluated using R^2, root mean squared error (RMSE), and mean average error (MAE) as metrics to assess how well they would perform in production.

3. Results

3.1. *Field sampling data*

The yield of *Parkia biglobosa* fruits ranged from 4.0 kg to 218.0 kg per tree, with a median yield of 56.0 kg and an average yield of 57.0 kg. The highest and lowest yields were recorded in Kumbungu, where the median yield was 26.5 kg, and the average yield was 37.6 kg. The yield from Nandom ranged from 27.0 to 139.0 kg with a median of 68.0 kg and an average of 69.5 kg. The yield from Navrongo ranged from 10.0 to 90.0 kg with a median of 64.0 kg and an average of 57.3 kg (Fig. 2a).

Generally, crown areas range from 23.87 to 524.6 m^2 per tree. The median and average crown areas were 167.9 and 180.3 m^2 per tree, respectively. In Kumbungu, the crown areas varied from 70.3 to 511.6 m^2 per tree, with a median and mean of 174.1 and 203.5 m^2 per tree, respectively. The range of values from Nandom was 30.5 to 524.6 m^2 per tree, with median and mean values of 173.3 and 179.5 m^2 per tree, respectively. Values from Navrongo were from 23.9 to 291.8 m^2 per tree with median and mean values of 145.6 and 151.0 m^2 per tree, respectively, Fig. 2(b). Thus, the largest and smallest tree crowns were found in Nandom and Navrongo, respectively.

3.2. *Relationships modelling*

3.2.1. *Selection of models*

The interactive-form models (models with interaction terms) that were used to explain the yield in the training data accounted for 53.7 % to 64.4 % of the variation in yield (Appendix Table A). The interaction terms improved model performance (increased R^2), showing that the yield relies on a combination of factors. Integrating drone and satellite-based data also improved model performance. Models using only drone (Model 3.4, R^2 = 63.1%) and satellite (Model 3.5, R^2 = 63.0%) each improved over the soil property baseline (Model 3.1, R^2 = 60.9%). Model 3.6, which integrated drone and satellite-based data, achieved the highest R^2 = 64.4%, thus explaining an additional 1.3-1.4% variance (Appendix Table A).

The basic-form models (models with no interaction terms) showed progressive improvement in their ability to explain variation in yield from the training data. Model 4.5 exhibited the highest explanatory power of 60.9 % in the training data. The model incorporated the natural log of crown radius, drone NGRDI, N, and CEC[F] at 100–200 cm depth and accounted for location effect (Appendix Table B).

3.2.2. *Model validation*

The RMSE values for interactive-form models (model 3.1- 3.6) ranged from 0.38 to 0.45 and MAE from 0.28 to 0.36. Model 3.3 was the highest performing model in the group. It achieved an RMSE of 0.37 and an MAE of 0.31 (Appendix Table C). With the highest R^2 of 75 %, it indicated a better fit and stronger predictive capability (Fig. 3A). The interactive terms enhanced the predictive accuracy; thus, the interaction effect is important in *Parkia biglobosa* yield prediction.

The RMSE values of the basic-form models (model 4.1-4.5) ranged from 0.43 to 0.46, their MAE values were between 0.34 and 0.39, and R^2 values ranged from 63 % to 68 % (Appendix Table D). Model 4.4 achieved the best fit in the validation data, with RMSE of 0.43, MAE of 0.34, and R^2 of 68 % (Fig. 3B).

3.2.3. *Model coefficients*

The coefficient of the natural logarithm of the crown radius, i.e., ln (r), consistently exhibited a positive effect on yield across all models. In interactive-form models, the effect of Nitrogen varied across location: it was consistently negative in Navrongo, variable in Nandom, and positive in Kumbungu (Appendix Table E). Variables such as Sand and the average of the blue spectral bands of drone and satellite images (B.x and B.y, respectively) also showed mixed significance across models. In the presence of Nitrogen interactions, CI.x and N were mostly impactful. Thus, yield is influenced by ln(r), effect of sand, spectral bands, and nitrogen interactions (Appendix Table E).

Among the interactive-form models, the best model was model 3.3, which indicated that yield depended on the combination of the base factor and the response to crown radius (r), average blue (B.y) from satellite images, location-specific effects, and interactions with B.y. There was a strong balance between model fit (AIC = 126.3), explanatory power (R^2 = 75 %), and predictive accuracy (RMSE = 0.377, MAE = 0.308) (Appendix Table A, Table C). The exponentiated equation was

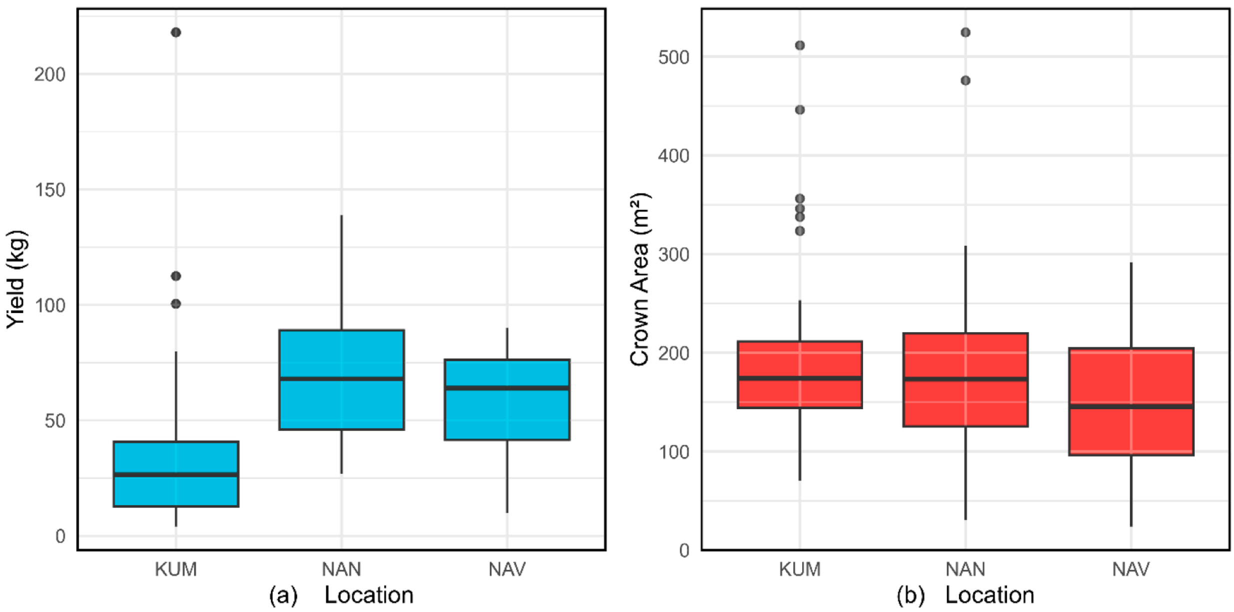

Fig. 2. Overview of yield (a) and crown area (b) in the three study areas.

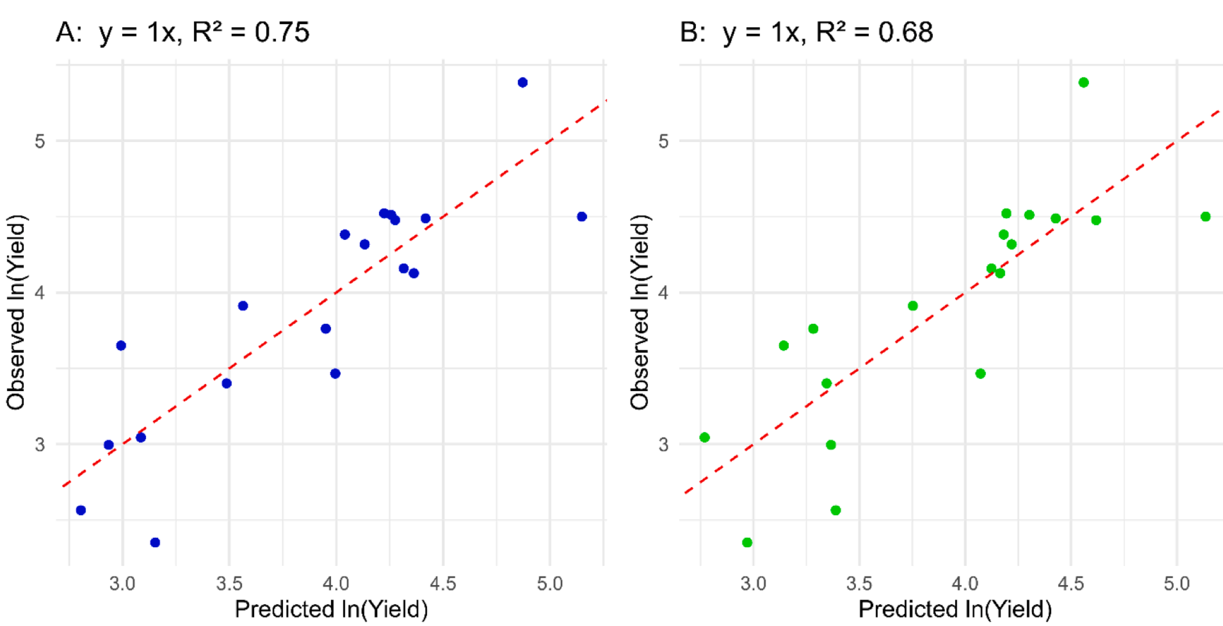

Fig. 3. Regression of natural logarithm values of observed yield of Parkia biglobosa pods on their predicted values.

stated as:

$$Y_j = e^{5.322} \cdot r^{1.037} \cdot e^{-0.008 \cdot B.y} \cdot (Location\ Effect)_j \tag{6}$$

Where:

$$Location\ Effect = \begin{cases} J = 1: & e^{-2.857+0.009 \cdot B.y}, & Nandom \\ J = 2: & e^{-5.975+0.013 \cdot B.y}, & Navrongo \\ J = 3: & 1, & Kumbungu \end{cases}$$

However, the most practically usefull model was derived from model 3.5. It declined in explanatory power ($R^2 = 72.6$ %) with a marginal increase in outliers (RMSE = 0.394) but improved in predictive accuracy (MAE = 0.284) compared to model 3.3 (Appendix Table C) It describes yield as a function of crown radius (r), satellite NIR reflectance (N), soil Nitrogen at depth 60–100 cm (Nitrogen[E]), and Location (Appendix Table E)) and expressed as an exponential model (Equation 7).

$$Y_j = e^{-4.672} \cdot r^{0.907} \cdot e^{0.001N} \cdot (Location\ Effect)_j \tag{7}$$

Where

$$Location\ Effect = \begin{cases} J = 1: & e^{5.156-0.100\ \text{Nitrogen[E]}}, & Nandom \\ J = 2: & e^{11.275-0.327\ \text{Nitrogen [E]}}, & Navrongo \\ J = 3: & 1, & Kumbungu \end{cases}$$

The global coefficient $e^{(-4.672)}$ is about 0.0094, suggesting the intercept has little impact on yield, while the variables are the main determinants.

The effect of CEC[F] in the basic-form models was mostly similar, though negative. Nandom and Navrongo mostly showed positive impacts. Other variables such as NGRDI.x, pH[D], and N exhibited mixed significance (Appendix Table E).

The best basic-form model was model 4.4. The AIC was 119.3, R^2

67.8 %, RMSE 0.427, and MAE 0.340 (Appendix Table B, Table D). It indicated that yield depends on the combination of the base factor and the response to crown radius (r), near-infrared (N) from satellite images, soil pH at 30-60 cm depth (pH[D]), and location-specific effects (Appendix Table F). The exponentiated equation was stated as:

$$Y_j = e^{-15.699} \cdot r^{0.989} \cdot e^{0.001N+0.242pH[D]} \cdot (Location\ Effect)_j \tag{8}$$

Where:

$$Location\ Effect = \begin{cases} J=1: & e^{0.153}, & Nandom \\ J=2: & e^{-0.488}, & Navrongo \\ J=3: & 1, & Kumbungu \end{cases}$$

The global coefficient $e^{-15.699}$ is approximately 1.52×10^{-7}, a number close to zero, indicating that the intercept plays a minimal role in predicting yield. Thus, the effects of the variables are the major determinants of yield.

4. Discussion

4.1. Field sampling data

Tree production varied across the study sites. The range of values observed was closely aligned with previously reported ranges in the literature, 25-100 kg/tree by Pasiecznik, (2022) and 25-130 kg/tree by Houndonougbo et al., (2020), while others deviated significantly. The variation suggested that there could be differences in conditions and practices in production. These could be due to soil quality, climate, or vegetation health conditions not considered. The range widens, 0.25-200 kg/tree, when climate and management practices are taken into consideration (Bokary et al., 2022).

The variability of canopy areas of *Parkia biglobosa* across the study sites points to the influence of management and environmental factors on tree growth. Areas with higher mean precipitation exhibited larger canopy areas, suggesting that moisture availability impacts canopy growth. They could also be due to differences in soil factors (Alo and Aweto, 2018). The canopy sizes observed in this study were consistent with reports on canopy diameter of 12-19 m, which approximately range from 113-284 m^2, assuming circular canopies.

4.2. Relationship modeling

Yield is influenced by an interplay of physical, biological, and environmental factors. The exponential relationship between tree traits, as depicted in the global term, has been extensively used in allometric studies and yield predictions (Chave et al., 2014; Duncanson et al., 2015; Liu et al., 2023; Peters et al., 1988). The results of the global term have been enhanced by incorporating climate (Ounyambila et al., 2018), soil, and management practices (Madin and Nelson, 2023), each of which is considered separately. A more comprehensive approach is adopted in this study by combining soil, tree health, and effects of locality on the global term in a generalized exponential framework to improve results over earlier approaches. The model's predictive ability may be limited by the non-inclusion of higher-order terms for spectral and soil variables. However, capturing such non-monotonic responses in spectral and soil variables may also increase complexity and come at the cost of interpretability and operational usability in the field

In respect of *Parkia biglobosa,* Bokary et al., (2022) found that yield is significantly explained by crown diameter (or radius) in a linear relationship. In this study, it was observed that the relationship is not linear, but nonlinear with a power close to 1. When interaction terms are not considered, it increases with increasing crown size at a decreasing rate ($n = 0.989$). In contrast, when interaction terms are considered, the relationship becomes more dynamic; it either increases at an increasing rate ($n = 1.037$) or continues to increase at a decreasing rate ($n=0.907$), depending on the purpose of the model. A more extreme nonlinear effect (about twice) was observed in shrubs of the Sudanian zone (*Ximenia americana*), where yield grows at an increasingly faster rate as crown radius increases (Ounyambila et al., 2018). This could be explained by differences in physical and biological properties, since trees and shrubs may respond to environmental and management factors in unique ways.

The near-linear relationships observed could be explained by age of the tree branches, harvesting practices, and environmental stressors. Younger branches tend to produce more fruits, while older ones experience reduced fruit-bearing capacity due to physiological changes, reduced nutrient flow, and diminished utility (Boffa, 1999; Zhou and Melgar, 2020). Branch age correlates with the location, angle, and order in the overall crown structure. Younger branches are at the tips or in zones of active growth where there is abundant sunlight for photosynthesis and high carbon export ability, with a lower wood-to-leaf biomass ratio to improve fruit yield. The older branch portions are less productive because they are longer, have a higher wood-to-leaf biomass ratio, and a reduced ability to export carbon to the fruits (Rosati et al., 2018). Again, Common harvesting practices that use sickle blades to cut off fruit-bearing branch tips create scars, which lead to reduced fruit production. Environmental stressors further increase yield loss in *Parkia biglobosa*. For instance, bushfires decrease fruit yield by burning the canopy, leading to the loss of leaves, flowers, and young fruits. This reduction in leaf area diminishes photosynthetic capacity and activity, resulting in less carbohydrates available for fruit development. The soil degradation after fires further hampers recovery.

Improvements in models 3.3 and 4.4, achieved by adding soil conditions and/or satellite spectral characteristics to the structural trait of *Parkia biglobosa*, led to better yield predictions. Compared to the linear model from Bokary et al., (2022), the over 67 % explanatory power suggests that it is capturing complexities effectively. It, however, agrees with his assertion that *Parkia biglobosa* crown diameter (or radius) is a good predictor of its fruit yield. Compared to similar non-linear models for predicting yield in distinct climates ($R^2 = 46.0$ %) (Ounyambila et al., 2018), an R^2 margin of improvement between 21 and 29 percentage points was observed.

Integrating drone and satellite data improved model performance and reduced location biases compared to using only one of the two data sources. The drone images provided high spatial resolution and detailed canopy structure. They captured two-dimensional variation in crown geometry, leaf density, and fruit distribution. The satellite images had lower spatial resolution but included near-infrared bands that distinguished canopy health and stress that were not visible in RGB drone imagery. The combination enhanced canopy characterization.

Rice nitrogen-use efficiency is higher in tropical regions than in temperate ones (Chen et al., 2023), while wheat yields benefit more from nitrogen in cooler climates (Yokamo et al., 2023). Therefore, soil nitrogen impacts yields variably across locations. A similar observation was made in this study, as Nitrogen positively affects Kumbungu (+0.110) but negatively impacts Nandom (-0.100) and Navrongo (-0.327) in model 3.5. Similarly, in model 3.6, its impact on Kumbungu is positive (+0.159), while Nandom (-0.149) and Navrongo (-0.310) are negative (Appendix Table E). This variation can be attributed to the climate gradient across the study sites.

The exponential expressions (7) and (8) have global coefficients close to zero. The observed small intercepts are biologically realistic and suggest that yield depends on structural and environmental factors. A tree with zero crown radius, no spectral response, and average soil input will produce zero yield. Thus, there is no constant yield even when biophysical drivers are absent.

5. Conclusions and recommendations

The yield of *Parkia biglobosa* is influenced by its crown radius, soil properties, spectral characteristics, and location-specific variations in a non-linear relationship. Integrating these factors leads to a more accurate prediction of yield, which can inform better decision-making and yield optimization strategies.

Combining drone and satellite-based spectral variables with soil and crown metrics improved model performance and practical relevance by reducing prediction errors. The interaction terms improved model accuracy by capturing variations due to location-specific soil and environmental conditions. Specifically, it increased explanatory power and improved the prediction errors. Yield responses intended for large-scale application are best represented when spatial and environmental interactions are explicitly modeled.

Including interaction terms shows that yield growth relative to crown radius can either increase or decrease, highlighting the importance of considering the influence of local environmental factors, which can modify the crown radius-yield relationship differently across regions. Nitrogen has specific location effects influencing yield, suggesting that tailored management practices are required to optimize yield.

The model is applicable in scenarios where multiple variables influence yield. In regional yield studies with field measurements from drones, satellite imagery, and soil parameters, the images can be used to estimate crown radius, and then the model can be used to capture the nonlinear dynamics, providing a more realistic forecast.

In addition, location-specific management practices should be implemented to optimize soil health and enhance the accuracy of large-scale *Parkia biglobosa* yield predictions by leveraging spectral indices derived from remote sensing. To maintain yield estimates, targeted policies are needed for bushfire control, less invasive harvesting techniques, and monitoring of nitrogen levels, soil pH, and tree crown radius. Effective bushfire management and undergrowth protection training are vital for tree health and productivity.

It is recommended for future research to investigate computational frameworks that consider monotonic predictors, incorporating non-linear effects.

Funding Information

This work is funded by the Ministry of Foreign Affairs of Denmark and administered by the Danida Fellowship Centre through the Climate Change Resilience of Ecosystem Services (CRES) Project with Grant No. DFCFileNO.20-13-GHA.

CRediT authorship contribution statement

Franklin X. Dono: Writing – original draft, Methodology, Investigation, Formal analysis, Conceptualization. **Bernard N. Baatuuwie:** Writing – review & editing, Supervision, Methodology, Conceptualization. **Anne Mette Lykke:** Writing – review & editing, Supervision, Methodology, Conceptualization. **Felix K. Abagale:** Writing – review & editing, Supervision, Methodology, Conceptualization. **Peter Borgen Sørensen:** Writing – review & editing, Supervision, Methodology, Formal analysis, Conceptualization.

Declaration of competing interest

The authors declare that they have no conflicts of interest.

Acknowledgments

The authors thank the West African Centre for Water, Irrigation and Sustainable Agriculture (WACWISA) and the University for Development Studies, Ghana, for providing the necessary support to conduct this study.

Appendix

Applied models

A. Models with interaction terms

$$\ln(yield) = \beta_0' + n \times \ln(r) + \beta_1 \times soil + \beta_2 \times Location + \beta_3 \times soil \times Location \tag{3.1}$$

$$\ln(yield) = \beta_0' + n \times \ln(r) + \beta_1 \times drone + \beta_2 \times Location + \beta_3 \times drone \times Location \tag{3.2}$$

$$\ln(yield) = \beta_0' + n \times \ln(r) + \beta_1 \times satellite + \beta_2 \times Location + \beta_3 \times satellite \times Location \tag{3.3}$$

$$\ln(yield) = \beta_0' + n \times \ln(r) + \beta_1 \times drone + \beta_2 \times soil + \beta_3 \times Location + \beta_4 \times soil \times Location \tag{3.4}$$

$$\ln(yield) = \beta_0' + n \times \ln(r) + \beta_1 \times satellite + \beta_2 \times soil + \beta_3 \times Location + \beta_4 \times soil \times Location \tag{3.5}$$

$$\ln(yield) = \beta_0 + n \times \ln(r) + \beta_1 \times drone + \beta_2 \times satellite + \beta_3 \times soil + \beta_4 \times Location + \beta_5 \times soil \times Location \tag{3.6}$$

B. Models with no interaction terms

$$\ln(yield) = \beta_0' + n \times \ln(r) + \beta_1 \times Location \tag{4.1}$$

$$\ln(yield) = \beta_0' + n \times \ln(r) + \beta_1 \times soil + \beta_2 \times Location \tag{4.2}$$

$$\ln(yield) = \beta_0' + n \times \ln(r) + \beta_1 \times drone + \beta_2 \times soil + \beta_3 \times Location \tag{4.3}$$

$$\ln(yield) = \beta_0' + n \times \ln(r) + \beta_1 \times satellite + \beta_2 \times soil + \beta_3 \times Location \tag{4.4}$$

C Repeated random sampling with holdout for final validation

The data was divided into two parts: 80 % for training and 20 % for final validation, and a balanced representation from each location was ensured. Using 80 % of the training dataset, we sampled a balanced representation repeatedly over 4000 iterations to build models. The Akaike information criterion was used in each iteration to select the best model, which was stored. After all iterations were completed, the most frequently occurring model was selected. The selected model was validated using the reserved validation dataset to assess its performance. The process was implemented using the caret package for data partitioning, while the lm() function in R was used for fitting the linear models.

Tables

Table A
Summary of performance metrics of interactive-form models for estimation of fruit yield.
The table summarizes the performance of models for predicting the yield of *Parkia biglobosa pods* considering interactions terms. The variables B.x and B.y represent average spectral reflectance values obtained from drone and satellite images, respectively. [D] and [E] denote soil depth intervals of 30–60 cm and 60–100 cm, respectively.

Model	Formula: ln(Yield) ~	Weight (%)	Mean AIC	Mean R^2 (%)	SD R^2
3.1	ln(r) + Sand[D] * Location	48.0	115.1	60.9	0.042
3.2	ln(r) + B.x * Location	62.2	127.8	53.7	0.046
3.3	ln(r) + B.y * Location	66.4	126.3	55.4	0.039
3.4	ln(r) + NGRDI.x + Sand[D] * Location	21.2	112.5	63.1	0.039
3.5	ln(r) + N + Nitrogen[E] * Location	24.8	114.0	63.0	0.050
3.6	ln(r) + CI.x + N + Nitrogen[E] * Location	19.4	115.0	64.4	0.051

Table B
Summary of performance metrics of basic-form models for estimation of fruit yield.
The table summarizes the performance of models for predicting yield of *Parkia biglobosa* pods without considering interaction terms. [D] and [F] refers to soil depth intervals of 30–60 cm and 100–200 cm, respectively.

Model	Formula: ln(Yield) ~	Weight (%)	Mean AIC	Mean R^2 (%)	Std. R^2
4.1	ln(r) + Location	100	138.2	42.5	-
4.2	ln(r) + CEC[F] + Location	48.8	122.1	55.1	0.040
4.3	ln(r) + NGRDI.x + CEC[F] + Location	47.6	119.6	58.2	0.038
4.4	ln(r) + N + pH[D] + Location	38.5	119.3	58.1	0.049
4.5	ln(r) + NGRDI.x + N + CEC[F] + Location	28.1	117.6	60.9	0.035

Table C
Validation metrics for interactive-form models.

Model	R^2 (%)	RMSE	MAE
3.1	65.2	0.444	0.345
3.2	64.5	0.449	0.357
3.3	75.0	0.377	0.308
3.4	67.1	0.432	0.331
3.5	72.6	0.394	0.284
3.6	67.7	0.428	0.350

Table D
Validation metrics for basic-form models.

Model	R^2 (%)	RMSE	MAE
4.1	62.9		
4.2	62.9	0.459	0.389
4.3	64.9	0.446	0.372
4.4	67.8	0.427	0.340
4.5	64.9	0.446	0.370

Table E
Coefficients table for interactive-form models.
The table summarizes the coefficients of models for predicting the yield of *Parkia biglobosa* pods with interaction terms. Soil depth intervals are represented as [A]: 0–5 cm, [B]: 5–15 cm, [C]: 15–30 cm, [D]: 30–60 cm, [E]: 60–100 cm, and [F]: 100–200 cm.

Term	Estimate	Std. Error	P. Value	Significance
Model 3.1: ln(Yield) ~ ln(r) + Sand[D] * Location				
(Intercept)	-0.581	0.864	0.503	
ln(r)	1.026	0.210	0.000	***
Sand[D]	0.005	0.002	0.013	*
LocationNandom	4.824	6.737	0.476	
LocationNavrongo	-13.572	4.310	0.002	**
Sand[D]: LocationNandom	-0.009	0.014	0.540	
Sand[D]: LocationNavrongo	0.031	0.010	0.001	**
Model 3.2: ln(Yield) ~ ln(r) + B.x * Location				
(Intercept)	1.392	0.475	0.004	**
ln(r)	1.198	0.215	0.000	***
B.x	-0.004	0.004	0.330	
LocationNandom	0.522	0.697	0.456	
LocationNavrongo	-2.529	0.982	0.012	*
B.x: LocationNandom	0.011	0.015	0.453	
B.x: LocationNavrongo	0.050	0.014	0.001	**
Model 3.3: ln(Yield) ~ ln(r) + B.y * Location				
(Intercept)	5.322	1.584	0.001	**
ln(r)	1.037	0.215	0.000	***
B.y	-0.008	0.003	0.009	**
LocationNandom	-2.857	1.793	0.114	
LocationNavrongo	-5.975	1.740	0.001	**
B.y: LocationNandom	0.009	0.004	0.024	*
B.y: LocationNavrongo	0.013	0.003	0.000	***
Model 3.4: ln(Yield) ~ ln(r) + NGRDI.x + Sand [D] * Location				
(Intercept)	-0.881	0.888	0.324	
ln(r)	1.086	0.214	0.000	***
NGRDI.x	-2.485	1.811	0.173	
Sand[D]	0.006	0.002	0.005	**
LocationNandom	4.942	6.707	0.463	
LocationNavrongo	-13.654	4.291	0.002	**
Sand[D]: LocationNandom	-0.010	0.014	0.497	
Sand[D]: LocationNavrongo	0.031	0.010	0.001	**
Model 3.5: ln(Yield) ~ ln(r) + N + Nitrogen [E] * Location				
(Intercept)	-4.672	1.744	0.009	**
ln(r)	0.907	0.213	0.000	***
N	0.001	0.000	0.113	
Nitrogen[E]	0.110	0.033	0.001	**
LocationNandom	5.156	1.798	0.005	**
LocationNavrongo	11.275	2.389	0.000	***
Nitrogen[E]: LocationNandom	-0.100	0.043	0.024	*
Nitrogen[E]: LocationNavrongo	-0.327	0.081	0.000	***
Model 3.6: ln(Yield) ~ ln(r) + CI.x + N + Nitrogen [E] * Location				
(Intercept)	-6.049	1.801	0.001	**
ln(r)	0.946	0.209	0.000	***
CI.x	-2.420	1.025	0.020	*
N	0.001	0.000	0.014	*
Nitrogen[E]	0.159	0.039	0.000	***
LocationNandom	6.902	1.906	0.000	***
LocationNavrongo	11.207	2.335	0.000	***
Nitrogen[E]: LocationNandom	-0.149	0.047	0.002	**
Nitrogen[E]: LocationNavrongo	-0.310	0.080	0.000	***

Where p. value < 0.001: ***, p. value < 0.01: **, p. value < 0.05: *, p. value < 0.1: .

Table F
Coefficient table for basic-form models.
The table summarizes the coefficients of models for predicting yield of *Parkia biglobosa* pods without interaction terms. Soil depth intervals are represented as [A]: 0–5 cm, [B]: 5–15 cm, [C]: 15–30 cm, [D]: 30–60 cm, [E]: 60–100 cm, and [F]: 100–200 cm.

Term	Estimate	Std. Error	P.Value	Significance
Model 4.1: ln(Yield) ~ ln(r) + Location				
(Intercept)	-1.552	1.182	0.209	
ln(r)	2.898	0.674	0.001	***
LocationNandom	0.884	0.275	0.006	**

(*continued on next page*)

Table F (*continued*)

Term	Estimate	Std. Error	P.Value	Significance
Model 4.1: ln(Yield) ~ ln(r) + Location				
LocationNavrongo	1.082	0.359	0.009	**
Model 4.2: ln(Yield) ~ ln(r) + CEC[F] + Location				
(Intercept)	4.148	1.032	0.000	***
ln(r)	1.166	0.211	0.000	***
CEC[F]	-0.021	0.007	0.002	**
LocationNandom	0.721	0.171	0.000	***
LocationNavrongo	0.836	0.161	0.000	***
Model 4.3: ln(Yield) ~ ln(r) + NGRDI.x + CEC[F] + Location				
(Intercept)	5.035	1.179	0.000	***
ln(r)	1.228	0.213	0.000	***
NGRDI.x	-2.906	1.912	0.132	
CEC[F]	-0.026	0.007	0.001	**
LocationNandom	0.369	0.287	0.202	
LocationNavrongo	0.714	0.179	0.000	***
Model 4.4: ln(Yield) ~ ln(r) + N + pH[D] + Location				
(Intercept)	-15.699	4.205	0.000	***
ln(r)	0.989	0.215	0.000	***
N	0.001	0.000	0.016	*
pH[D]	0.242	0.070	0.001	**
LocationNandom	0.153	0.351	0.664	
LocationNavrongo	-0.488	0.503	0.334	
Model 4.5: ln(Yield) ~ ln(r) + NGRDI.x + N + CEC[F] + Location				
(Intercept)	2.279	1.737	0.193	
ln(r)	1.101	0.218	0.000	***
NGRDI.x	-3.712	1.916	0.056	.
N	0.001	0.000	0.036	*
CEC[F]	-0.023	0.007	0.002	**
LocationNandom	0.501	0.289	0.086	.
LocationNavrongo	0.879	0.192	0.000	***

Where p. value < 0.001: ***, p. value < 0.01: **, p. value < 0.05: *, p. value < 0.1:

Data availability

Data will be made available on request.

References

Alo, E.A., Aweto, A.O., 2018. The properties of soil under the canopy of the locust bean tree (Parkia biglobosa), in relation to Tree Biomass , in Farmland in Oyo Area , South Western Nigeria. J. Environ. Earth Sci. 8 (8), 38–46.

Apolo-Apolo, O.E., Martínez-Guanter, J., Egea, G., Raja, P., Pérez-Ruiz, M., 2020. Deep learning techniques for estimation of the yield and size of citrus fruits using a UAV. Eur. J. Agron. 115, 126030. https://doi.org/10.1016/j.eja.2020.126030.

Area, C. P., & Photographs, L. S. (2004). Chapter 6 Estimating crown projected area from remote sensing at different spatial resolution and its use in estimating DBH. 78–149.

Asad Naqvi, S.A., Naqvi, R.Z., 2022. Geographical information systems (GIS) in industry 4.0: revolution for sustainable development. Handbook of Smart Materials, Technologies, and Devices: Applications of Industry 4.0: Volume 1-3, pp. 2289–2315. https://doi.org/10.1007/978-3-030-84205-5_83, 3.

Ayanrinde, F.A., Oyewole, S.O., Ayanrinde, O.A., Oyewole, A.L., 2023. Importance of Parkia biglobosa (African Locust Beans) to the women livelihoods in Ibarapa North and Ibarapa central local government Areas of Oyo State, Nigeria. J. Appl. Sci. Environ. Manag. 27 (9), 2097–2100. https://doi.org/10.4314/jasem.v27i9.27.

Barbosa, B.D.S., Ferraz, G.A.e.S., Costa, L., Ampatzidis, Y., Vijayakumar, V., dos Santos, L.M., 2021. UAV-based coffee yield prediction utilizing feature selection and deep learning. Smart Agric. Technol. 1, 100010. https://doi.org/10.1016/j.atech.2021.100010.

Boffa, J.-M., 1999. Improved Parkland Management. Agroforestry Parklands in Sub-Saharan Africa. Food and Agriculture Organization of the United Nations.

Bokary, A.K., Amadou Malé, K., Sidiki, G.D., 2022. Effect of climatic zone and land use practices on pod, seed and pulp yield of Parkia biglobosa in Southern Mali. Int. J. Sci. Res. Updates 4 (1), 312–321. https://doi.org/10.53430/ijsru.2022.4.1.0138.

Chave, J., Réjou-Méchain, M., Búrquez, A., Chidumayo, E., Colgan, M.S., Delitti, W.B.C., Duque, A., Eid, T., Fearnside, P.M., Goodman, R.C., Henry, M., Martínez-Yrízar, A., Mugasha, W.A., Muller-Landau, H.C., Mencuccini, M., Nelson, B.W., Ngomanda, A., Nogueira, E.M., Ortiz-Malavassi, E., Vieilledent, G., 2014. Improved allometric models to estimate the aboveground biomass of tropical trees. Glob. Change Biol. 20 (10), 3177–3190. https://doi.org/10.1111/gcb.12629.

Chen, S., Elrys, A.S., Zhao, C., Cai, Z., Zhang, J., Müller, C., 2023. Global patterns and controls of yield and nitrogen use efficiency in rice. Sci. Total. Environ. 898, 165484. https://doi.org/10.1016/j.scitotenv.2023.165484.

Dronelink, I., 2022. Dronelink Softw.

Duncanson, L., Rourke, O., Dubayah, R., 2015. Small sample sizes yield biased Allometric equations in temperate forests. Sci. Rep. 5, 1–13. https://doi.org/10.1038/srep17153.

Duursma, R.A., Mäkelä, A., 2007. Summary models for light interception and light-use efficiency of non-homogeneous canopies. Tree Physiol. 859–870.

Garden, B., 2017. Crown and leaf traits as predictors of subtropical tree sapling growth rates. Plant Ecol. 10 (1), 136–145. https://doi.org/10.1093/jpe/rtw041.

Harris, I., Osborn, T.J., Jones, P., Lister, D., 2020. Version 4 of the CRU TS monthly high-resolution gridded multivariate climate dataset. Sci. Data 7 (1), 1–18. https://doi.org/10.1038/s41597-020-0453-3.

Hauser, L.T., Timmermans, J., van der Windt, N., Sil, Â.F., César de Sá, N., Soudzilovskaia, N.A., van Bodegom, P.M., 2021. Explaining discrepancies between spectral and in-situ plant diversity in multispectral satellite earth observation. Remote Sens. Environ. 265. https://doi.org/10.1016/j.rse.2021.112684. March.

Houborg, R., Fisher, J.B., Skidmore, A.K., 2015. Advances in remote sensing of vegetation function and traits. Int. J. Appl. Earth. Obs. Geoinf. 43, 1–6. https://doi.org/10.1016/j.jag.2015.06.001.

Houndonougbo, J.S.H., Kassa, B., Mensah, S., Salako, V.K., Glèlè Kakaï, R., Assogbadjo, A.E., 2020. A global systematic review on conservation nd domestication of Parkia biglobosa (Jacq.) R. Br. ex G. Don, an indigenous fruit tree species in Sub-Sahara African traditional parklands: current knowledge and future directions. Genet. Resour. Crop. Evol. 67 (4), 1051–1066. https://doi.org/10.1007/s10722-020-00892-w.

Komolafe, K., Olaleye, M.T., Huang, H.C., Pacurari, M., 2024. Contemporary insights into the biological mechanisms of Parkia Biglobosa. Int. J. Environ. Res. Public Health 21 (4). https://doi.org/10.3390/ijerph21040394.

Liu, B., Bu, W., Zang, R., 2023. Improved allometric models to estimate the aboveground biomass of younger secondary tropical forests. Glob. Ecol. Conserv. 41, e02359. https://doi.org/10.1016/j.gecco.2022.e02359. October 2022.

Ma, X., Mahecha, M.D., Migliavacca, M., van der Plas, F., Benavides, R., Ratcliffe, S., Kattge, J., Richter, R., Musavi, T., Baeten, L., Barnoaiea, I., Bohn, F.J., Bouriaud, O., Bussotti, F., Coppi, A., Domisch, T., Huth, A., Jaroszewicz, B., Joswig, J., Wirth, C., 2019. Inferring plant functional diversity from space: the potential of Sentinel-2. Remote Sens. Environ. 233, 111368. https://doi.org/10.1016/j.rse.2019.111368. March.

Madin, M.B., Nelson, K.S., 2023. Effects of landscape simplicity on crop yield: a reanalysis of a global database. PLoS. One 18 (12 December), 1–16. https://doi.org/10.1371/journal.pone.0289799.

Nandom Municipal Assembly, 2016. Geology and Soils. Nandom District. https://www.nandomdistrict.gov.gh/2016/09/14/1-1-4-geology-and-soils/.

Ounyambila, L., Anne, M.L., Benjamin, L., Amadé, O., 2018. Influence of climate on fruit production of the yellow plum, Ximenia americana. Burkina Faso, West Africa J. Hortic. For. 10 (4), 36–42. https://doi.org/10.5897/jhf2017.0517.

Panagiotidis, D., Abdollahnejad, A., Surový, P., Chiteculo, V., 2017. Determining tree height and crown diameter from high-resolution UAV imagery. Int. J. Remote Sens. 38 (8–10), 2392–2410. https://doi.org/10.1080/01431161.2016.1264028.

Panda, S.S., Ames, D.P., Panigrahi, S., 2010. Application of vegetation indices for agricultural crop yield prediction using neural network techniques. Remote Sens. 2 (3), 673–696. https://doi.org/10.3390/rs2030673.

Pasiecznik, N., 2022. Parkia biglobosa (néré). CABI Compendium. https://doi.org/10.1079/cabicompendium.44162.

Peters, R.H., Cloutier, S., Dubé, D., Evans, A., Hastings, P., Kaiser, H., Kohn, D., Sarwer-Foner, B., 1988. The allometry of the weight of fruit on trees and shrubs in Barbados. Oecologia 74 (4), 612–616. https://doi.org/10.1007/BF00380061.

Poggio, L., De Sousa, L.M., Batjes, N.H., Heuvelink, G.B.M., Kempen, B., Ribeiro, E., Rossiter, D., 2021. SoilGrids 2.0: producing soil information for the globe with quantified spatial uncertainty. Soil 7 (1), 217–240. https://doi.org/10.5194/soil-7-217-2021.

Prado-Junior, J.A., Schiavini, I., Vale, V.S., Raymundo, D., Lopes, S.F., Poorter, L., 2016. Functional traits shape size-dependent growth and mortality rates of dry forest tree species. J. Plant Ecol. 10 (6). https://doi.org/10.1093/jpe/rtw103 rtw103.

Pretzsch, H., 2014. Forest ecology and management canopy space filling and tree crown morphology in mixed-species stands compared with monocultures. For. Ecol. Manag. https://doi.org/10.1016/j.foreco.2014.04.027.

Ribeiro da Luz, B., Crowley, J.K., 2010. Identification of plant species by using high spatial and spectral resolution thermal infrared (8.0-13.5 μm) imagery. Remote Sens. Environ. 114 (2), 404–413. https://doi.org/10.1016/j.rse.2009.09.019.

Rosati, A., Paoletti, A., Hariri, R.Al, Famiani, F., 2018. Fruit production and branching density a ff ect shoot and whole-tree wood to leaf biomass ratio in olive. Tree Physiol. 1278–1285. https://doi.org/10.1093/treephys/tpy009.

Soil Research Institute, 1999. Soil Map of Ghana. Land Suitability Section, Soil Research Institute, CSIR, Ghana.

Thomson, E.R., Malhi, Y., Bartholomeus, H., Oliveras, I., Gvozdevaite, A., Peprah, T., Suomalainen, J., Quansah, J., Seidu, J., Adonteng, C., Abraham, A.J., Herold, M., Adu-Bredu, S., Doughty, C.E., 2018. Mapping the leaf economic spectrum across West African tropical forests using UAV-Acquired hyperspectral imagery. Remote Sens. 10 (10). https://doi.org/10.3390/rs10101532.

Yiru, M., Ma, L., Zhang, Q., Huang, C., Yi, X., Chen, X., Hou, T., Lv, X., Zhang, Z., 2022. Cotton yield estimation based on vegetation indices and texture features derived from RGB image. Front. Plant Sci. 13 (June), 1–17. https://doi.org/10.3389/fpls.2022.925986.

Yokamo, S., Irfan, M., Huan, W., Wang, B., Wang, Y., Ishfaq, M., Lu, D., Chen, X., Cai, Q., Wang, H., 2023. Global evaluation of key factors influencing nitrogen fertilization efficiency in wheat : a recent meta-analysis (2000-2022). Front. Plant Sci. 1–17. https://doi.org/10.3389/fpls.2023.1272098. October.

Zhou, Q., Melgar, J.C., 2020. Tree age influences nutrient partitioning among annually removed aboveground organs of peach. HortScience 55 (4), 560–564. https://doi.org/10.21273/HORTSCI14731-19.